American Journal of Technology Advancement 2997-9382, Vol 3, No. 8, 2026

Article

Gaussian-Process Correction of Gas-Turbine Disc Crack-Initiation Life: A Computational Verification Study

Hadeel Raheem Jasim[1*]
Department of Materials Engineering, College of Engineering, University of Al-Qadisiyah, Al-Diwaniyah, Iraq
hadeel.raheem@qu.edu.iq

Hadeel Abdul Hassan Rahayf[2]
Department of Materials Engineering, College of Engineering, University of Al-Qadisiyah, Al-Diwaniyah, Iraq

Mudher Naeem Yasir[3]
Department of Materials Engineering, College of Engineering, University of Al-Qadisiyah, Al-Diwaniyah, Iraq

Abstract: Thermal-fatigue life prediction of gas-turbine discs is challenging because plasticity, creep, and progressive strain accumulation interact under extreme thermomechanical loading. This study compares constant-bias, linear, and Gaussian-process corrections applied to deformation-based crack-initiation life predictions for five disc cases. The correction inputs were maximum temperature and total strain range, and model performance was assessed through leave-one-disc-out evaluation. The uncorrected deformation criterion yielded a mean absolute error of 8.0 cycles and a root-mean-square error of 11.9 cycles. These values were reduced by Gaussian-process correction to 4.9 and 6.9 cycles, respectively, while the two-input linear model achieved lower errors of 2.2 and 2.4 cycles. Damage decomposition also revealed that in some discs, one-sided creep accumulation dominated while in other discs, cyclic-creep dominated, indicating that similar total damage can result from different mechanisms. The findings demonstrate the value of residual correction and highlight the importance of comparing Gaussian-process models with simpler alternatives in deformation-based disc-life prediction.

Keywords: gas-turbine disc; crack-initiation life; deformation criterion; Gaussian process; model discrepancy.

This is an open-access article under the CC-BY 4.0 license

1. Introduction

The discs of a gas turbine are subject to centrifugal loading, radial temperature gradients, high-temperature dwell, and repeated heating and cooling. Near attachment slots and fillets, these conditions create multiaxial and non-proportional stress–strain histories, including plasticity, creep, ratcheting, and progressive strain accumulation. A component-level study is thus focused on realistic geometry, temperature-dependent material properties and representative experimental loading when considering the assessment of crack initiation life [1][2][3][4].

Getsov used a thermocyclic disc test, three-dimensional thermo-elasto-viscoplastic finite element analysis and a deformation criterion that distinguished between cyclic plastic damage, cyclic creep damage, one-sided plastic accumulation and one-sided creep accumulation. The criterion gave a more accurate prediction of the crack initiation life than did the traditional Manson relation, though there were differences for some discs. These residual errors that drive the development of correction methods that retain the deformation-based prediction while accounting for systematic disagreement with experimental results.

Uncertainty associated with material properties, loading, geometry, fatigue–creep interaction, and finite-element response have been discussed in the context of probabilistic turbine-disc studies. Turbine disks and bladed-disk systems have been addressed using computational–experimental reliability frameworks, Monte Carlo procedures, stochastic uncertainty models and data-assisted creep–fatigue methods [5][6][7][8]. However, it is noted that these studies are not directly examine residual correction of the five deformation-based life predictions considered here.

Gaussian-process regression is a flexible probabilistic method for limited datasets [9]. It can also represent the discrepancy between numerical predictions and physical observations [10] and/or physical information may be introduced via the mean function, input variables, covariance structure, and/or multifidelity formulation [11][12].

Critical-plane quantities, multiaxial stress–strain variables, variable-amplitude test data, and physics-based constraints have all been applied to prediction of fatigue-life using Gaussian processes [13][14][15][16][17]. The purpose of Gaussian-process regression in the present study is not to replace the physical model of the material but to correct the residual difference between the experimental crack-initiation life and the deformation-based prediction.

This study compares constant-bias, linear, and Gaussian-process corrections using the same leave-one-disc-out procedure. It is a controlled five-case secondary-data comparison that distinguishes source observations from newly calculated results, examines kernel sensitivity, and evaluates whether the added complexity of Gaussian-process correction is justified for the available turbine-disc cases.

2. Methodology

The test results from the thermocycling and corresponding finite element calculations were taken from for five turbine discs. The selected cases (EN-1, EK-1, EK-2, No. 137, and No. 138) gave complete data on experimental crack-initiation life, deformation-criterion predictions, and damage components.

The summary of the principal source values is shown in Table 1.

Table 1. Experimental and Calculated Crack-Initiation Life of Turbine Discs.

Disc	Material	T_{max}, °C	Total strain range $\Delta\varepsilon$, %	N_{exp}, cycles	N_M, cycles	N_{def}, cycles
EN-1	EI612	620	1.00	40	6680	24
EK-1	EI481	620	1.40	75	228	54
EK-2	EI481	650	1.90	35	315	32
No. 137	EI765	800	1.05	7	1999	7
No. 138	EI765	750	1.10	13	174	13

In Table 1, T_max represents the maximum cycle temperature, Δε is the total strain range, N_exp is the experimentally observed crack-initiation life, N_M is the life predicted by the Manson relation, and N_def represents deformation-criterion life prediction.

The deformation criterion defines total damage as

$$D = D_1 + D_2 + D_3 + D_4, \qquad (1)$$

where D_1 represents the cyclic plastic damage, D_2 is cyclic creep damage, D_3 is one-sided plastic-accumulation damage, and D_4 represents one-sided creep-accumulation damage.

The finite-element deformation and damage values of the five discs are summarized in Table 2.

Table 2. Finite-Element Deformation and Damage at Crack Initiation.

Disc	$\Delta\varepsilon_{eq}^{p}$, %	$\Delta\varepsilon_{eq}^{c}$, %	ε_{eq}^{p}, %	ε_{eq}^{c}, %	D_1	D_2	D_3	D_4	D
EN-1	0.06	0.028	0.12	0.16	0.0073	0.101	0.032	1.570	1.71
EK-1	0.01	0.042	0.03	0.02	0.0004	0.409	0.150	0.871	1.43
EK-2	0.20	0.090	0.12	0.26	0.0067	0.526	0.029	0.520	1.09
No. 137	0.64	0.350	0.89	0.79	0.0530	0.620	0.070	0.250	1.01
No. 138	0.42	0.400	0.91	0.80	0.0790	0.659	0.180	0.140	1.06

In Table 1, $\Delta\varepsilon_{eq}^{p}$ and $\Delta\varepsilon_{eq}^{c}$ are the equivalent cyclic plastic- and creep-strain ranges, respectively, while ε_eq^p and ε_eq^c are the corresponding accumulated equivalent plastic and creep strains.

The deformation-criterion life was used as the physical-model baseline. The logarithmic residual for case i was set to be the natural logarithm:

$$r_i = \ln N_{exp,i} - \ln N_{def,i} = \ln\left(\frac{N_{exp,i}}{N_{def,i}}\right). \qquad (2)$$

where r_i is the logarithmic residual of case i, N_(exp,i) is the experimental crack-initiation life and N_(def,i) is the deformation-criterion prediction.

Four simple correction benchmarks were evaluated under leave-one-disc-out fitting:

1. a constant log bias correction;
2. a temperature only linear correction;
3. a strain-range only linear correction; and
4. a two-input linear correction.

For the constant-bias model, the omitted-case residual was estimated from the mean residual of the remaining cases:

$$\hat{r}_{i,\mathrm{bias}} = \frac{1}{n-1}\sum_{j\neq i} r_j \,. \qquad (3)$$

where r ˆ_(i,bias) denotes the estimated residual for the omitted case i, n denotes the total number of cases, and j indexes the training cases.

The two-input linear model was

$$r_i = \beta_0 + \beta_1 \tilde{T}_{\max,i} + \beta_2 \widetilde{\Delta\varepsilon}_i + e_i, \qquad (4)$$

where β_0 is the intercept; β_1 and β_2 are regression coefficients; T˜_(max,i) and (Δε)˜_i are the standardized maximum temperature and total strain range and e_i is the residual error.

Standardization is implemented by using the tilde, and the tilde with the training-fold mean and standard deviation. The one-input models were obtained by retaining only one predictor.

For Gaussian-process correction,

$$r(z) \sim \mathcal{GP}[0, k(z, z')], \qquad (5)$$

with the input vector

$$z_i = [T_{\max,i} \quad \Delta\varepsilon_i]^T. \qquad (6)$$

Here, GP denotes a Gaussian process, z_i is the input vector for case i, and the covariance function between input vectors z and z^' is given as k(z⓶,z^').

The maximum temperature and total strain range were selected as they were available for all cases. Other parameters, such as geometry, dwell-time and individual strain, were also omitted to prevent further over-parameterization.

A Matérn-3/2 covariance function was used:

$$k(z, z') = \sigma_f^2\left(1+\sqrt{3}q\right)\exp\left(-\sqrt{3}q\right) + \sigma_n^2\delta_{z,z'}, \qquad (7)$$

where

$$q = \sqrt{\sum_{j=1}^{2} \frac{\left(z_j - z_j'\right)^2}{\ell_j^2}}. \qquad (8)$$

In Eqs. (7) and (8) σ_f^2 is the process variance, σ_n^2 is the nugget variance, δ_(z,z^') is the K ronecker delta, q is the scaled distance between the input vectors, z_j and z_j^' are their jth components, and l_jis the characteristic length scale of input j.

The inputs were standardized within every training fold. Unrestricted hyperparameter optimization was not applied, as only four cases were left during each fit. The configuration selected set standardized length scales equal to one, the process variance to the sample variance of the training residuals and the nugget variance to 5% of that variance.

The corrected GP value was

$$\widehat{N}_{\mathrm{GP},i} = N_{\mathrm{def},i}\exp(\hat{r}_i), \qquad (9)$$

where N ˆ_(GP,i) is the GP-corrected crack-initiation life for case i, and r ˆ_i is the GP posterior mean in logarithmic space. The transformed value is the posterior median in cycle space.

and the nominal 95% interval was

$$N_{\mathrm{def},i}\exp(\hat{r}_i - 1.96s_i) \le N_i \le N_{\mathrm{def},i}\exp(\hat{r}_i + 1.96s_i), \qquad (10)$$

where s_i is the GP predictive standard deviation (in the logarithmic space), N_i is the unknown crack initiation life, and 1.96 is the standard normal multiplier that used for the nominal 95% interval.

The interval includes the nugget contribution of the fitted covariance model, but it does not represent all experimental, constitutive, or geometric uncertainty.

Leave one disc out verification was performed. In each iteration, four discs were used for model fitting and the omitted disc was used for evaluation. Prediction performance was quantified using the mean absolute error (MAE), root mean square error (RMSE), mean absolute percentage error (MAPE), coefficient of determination (R^2), mean absolute logarithmic error (E_log):

$$\mathrm{MAE} = \frac{1}{n}\sum_{i=1}^{n} | N_{\mathrm{exp},i} - \widehat{N}_i |, \qquad (11))$$

$$\mathrm{RMSE} = \sqrt{\frac{1}{n}\sum_{i=1}^{n}(N_{\mathrm{exp},i} - \widehat{N}_i)^2}, \qquad (12)$$

$$\mathrm{MAPE} = \frac{100}{n}\sum_{i=1}^{n}\left|\frac{N_{\mathrm{exp},i} - \widehat{N}_i}{N_{\mathrm{exp},i}}\right|, \qquad (13)$$

and

$$R^2 = 1 - \frac{\sum_i (N_{\mathrm{exp},i} - \widehat{N}_i)^2}{\sum_i (N_{\mathrm{exp},i} - \bar{N}_{\mathrm{exp}})^2}. \qquad (14)$$

and the mean absolute logarithmic error and the mean absolute logarithmic error

$$E_{\log} = \frac{1}{n}\sum_{i=1}^{n}\left|\ln \widehat{N}_i - \ln N_{\mathrm{exp},i}\right|. \qquad (15)$$

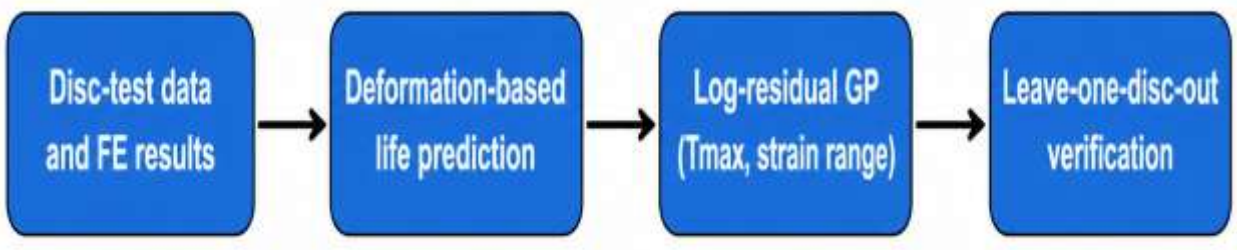
Spearman's rank correlation coefficient ϱ was also calculated to investigate the preservation of the experimental life ranking. In this case n=5 is the number of disc cases, N_(exp,i) is the experimental crack-initiation life for case i, N ̂_i is the corresponding predicted life, and ¯N_exp is the mean experimental crack-initiation life.

A compact sensitivity study was conducted to compare the performance of Matérn-3/2, Matérn-5/2, and radial-basis-function kernels using standardized length scales of 0.5, 1, and 2 and nugget fractions of 1%, 5%, and 10%. This resulted 27 fixed hyperparameter configurations.

Calculations were performed using Python 3.13.5, NumPy 2.3.5, pandas 2.2.3, SciPy 1.17.0, scikit-learn 1.8.0, and Matplotlib 3.10.8. No random initialization performed.

The overall GP procedure is summarized in Figure 1.

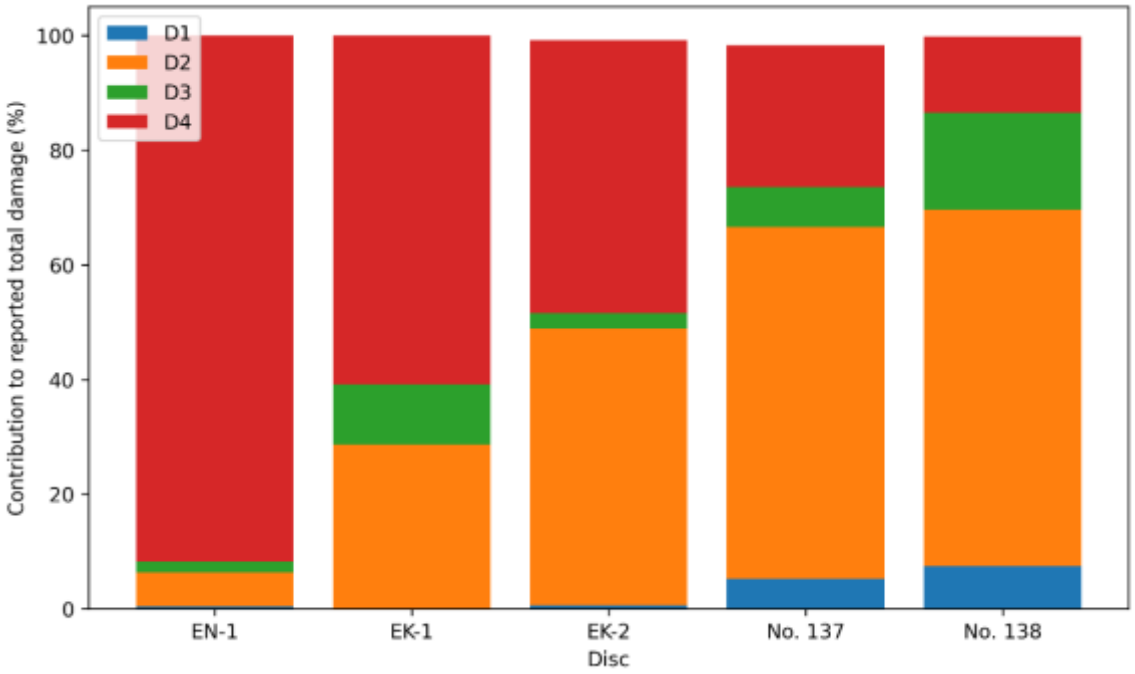
Figure 1. Gaussian-Process Correction Workflow for Disc-Life Prediction.



3. Results

The damage components were normalized by their displayed sum so each bar in Figure 2 equals 100%. One-sided creep accumulation D_4 accounted of 91.8% of the displayed damage components for EN-1 while 60.9% for EK-1. EK-2 was found to respond almost in balance, with cyclic creep D_2 accounting for 48.6% and one-sided creep accumulation accounting for 48.1%. Cyclic creep dominated No. 137 and No. 138 contributing 62.4% and 62.3% respectively.

Figure 2. Normalized Contributions of Finite-Element Damage Components.



The prediction metrics are shown in Table 3. The Manson relation strongly overpredicted life for these thermocyclic cases. The deformation criterion lowered the MAE to 8.0 cycles, and the RMSE to 11.9 cycles.

Table 3. Leave-One-Disc-Out Comparison of Life-Prediction Methods.

Method	MAE, cycles	RMSE, cycles	MAPE, %	R^2	Spearman ρ	$E_{\log}$
Manson relation	1845.2	3104.4	9459.9	−16683.69	0.00	3.335
Deformation criterion	8.0	11.9	15.3	0.756	0.90	0.186
Constant log-bias correction	7.1	8.5	23.0	0.874	0.90	0.234
Temperature-only linear correction	4.5	6.1	15.6	0.935	0.90	0.159
Strain-only linear correction	8.9	10.1	29.9	0.822	0.90	0.296
Two-input linear correction	2.2	2.4	9.4	0.990	1.00	0.096
Selected Matérn-3/2 GP correction	4.9	6.9	11.9	0.918	0.90	0.134

Relative to the uncorrected deformation criterion, the selected GP minimized the MAE by 38.9%, RMSE by 42.3%, MAPE by 22.3%, and mean absolute logarithmic error by 27.9%. But the two-input linear correction had the minimum errors and retained the full experimental ranking.

The experimental and calculated lives are compared in Figure 3. The vertical axis is logarithmic because the Manson predictions are very large compared to other values.

Figure 3. Experimental and Predicted Crack-Initiation Life with Residual Corrections.

The selected GP posterior medians and intervals are listed in Table 4.

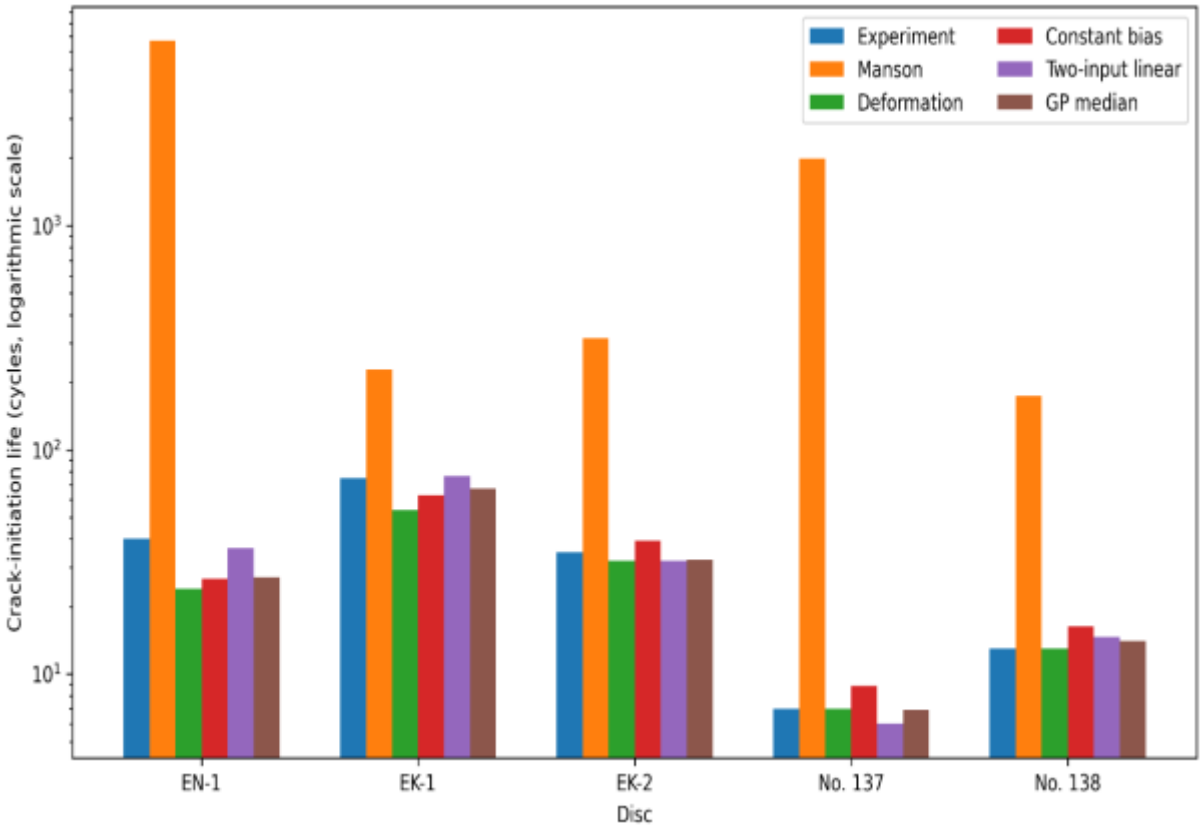


Table 4. Leave-one-disc-out Gaussian-process results

Disc	N_{exp}, cycles	N_{def}, cycles	GP prediction, cycles	Nominal 95% interval, cycles	Covered
EN-1	40	24	26.96	20.26–35.89	No
EK-1	75	54	67.47	44.07–103.30	Yes
EK-2	35	32	32.23	19.38–53.62	Yes
No. 137	7	7	6.93	4.62–10.41	Yes
No. 138	13	13	14.04	9.87–19.98	Yes

Four experimental results lay within their nominal intervals. This fraction is reported descriptively and is not treated as evidence of interval calibration.

The GP underestimated the life of EN-1 by 13.0 cycles and predicted a lower life for EN-1 compared with EK-2, but the experimental life of EN-1 was greater. This is a reversal that is why the GP reduced the magnitude-based errors while not improving the Spearman's rank correlation.

The leave-one-disc-out predictions and their nominal 95% intervals are compared against the experimental lives in Figure 4.

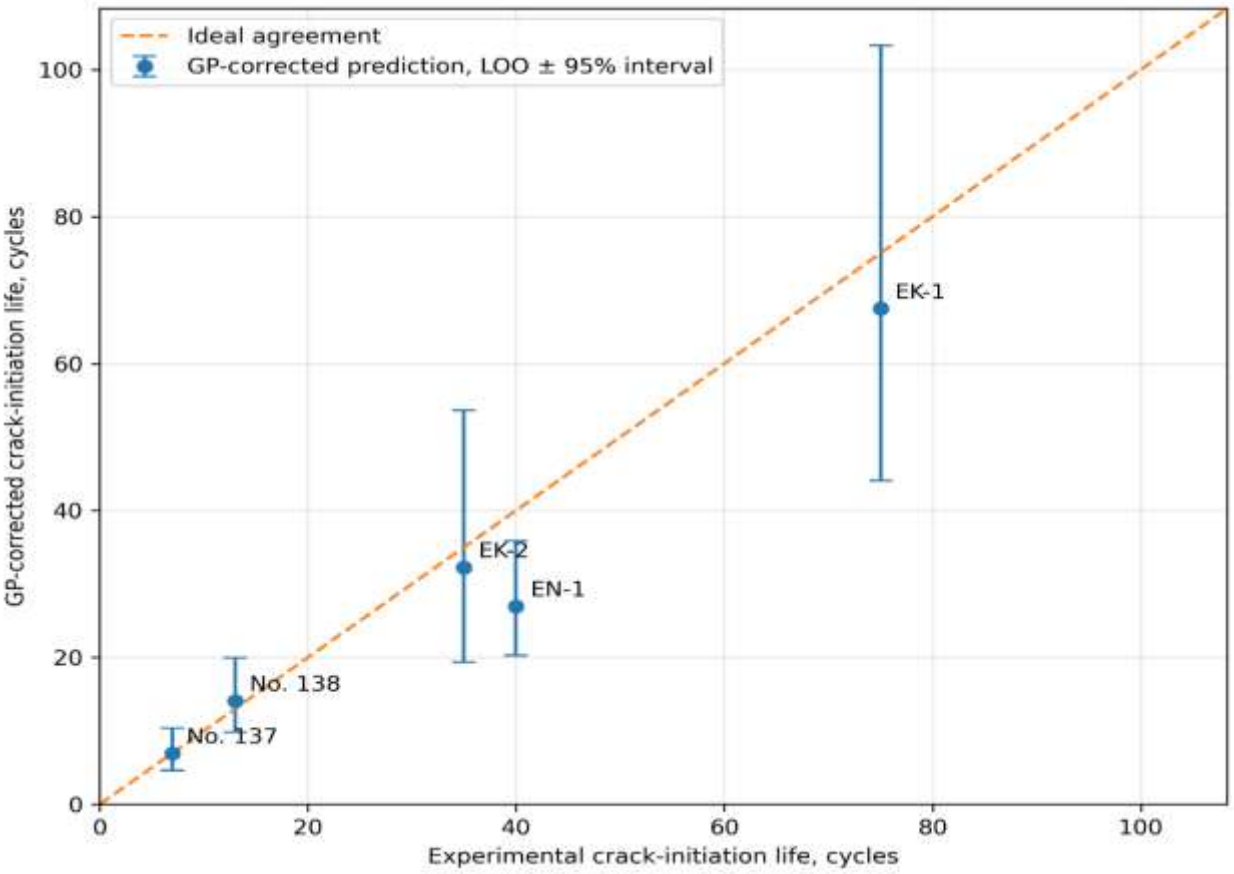


Figure 4. Gaussian-Process Predictions versus Experimental Crack-Initiation Life with 95% Intervals.

The sensitivity results are summarized in the following Table 5. Performance varied substantially with kernel and length scale, but changes in nugget fraction had smaller effect for a fixed kernel and length scale.

Table 5. Performance ranges across the fixed-hyperparameter sensitivity grid

Kernel	MAE range, cycles	RMSE range, cycles	MAPE range, %	Nominal coverage range, %
Matérn-3/2	2.7–7.3	4.7–10.6	9.3–14.4	80
Matérn-5/2	2.7–7.3	4.5–10.7	9.5–14.4	80
Radial basis function	2.6–7.4	4.1–10.9	9.9–14.4	60–80

The selected Matérn-3/2 configuration with unit-length scales and a 5% nugget fraction resulted in an MAE of 4.9 cycles and an RMSE of 6.9 cycles. In all 27 configurations, the MAE was between 2.6 and 7.4 cycles and RMSE was between 4.1 and 10.9 cycles, highlighting that conclusions depend materially on fixed kernel settings.

4. Discussion

The deformation criterion yielded much lower errors than Manson relation as it considered the effects of creep, multiaxial loading, non-proportional loading and progressive strain accumulation. The poor Manson predictions are therefore not a reflection of the general weakness of strain-life methods, but of the limited suitability of the method for these thermocyclic cases.

The damage decomposition revealed that the same total values of damage were obtained from different damage mechanisms. The one sided creep dominated in EN-1 and EK-1, while the mixed creep response was observed in EK-2 and the cyclic creep dominated in EI765 disc. This supports the use of mechanism-specific variables as well as total strain range.

The selected Gaussian-process (GP) correction reduced the error of the deformation criterion but was unable to outperform the two-input linear model. The linear model had an MAE of 2.2 cycles and an RMSE of 2.4 cycles, compared with 4.9 and 6.9 cycles for the GP. This is not a statement of general superiority of the linear model (as there are only 4 observations in each fitting fold), but an indication that the data available are not sufficient to support a unique advantage for the GP.

EN-1 was the most difficult case. The GP underestimated the life by 13.0 cycles and did not correct the ordering relative to EK-2, leaving a Spearman coefficient of 0.90. The limitations of the interpretation are also due to the fact that the materials, the geometry, the temperatures, the strain ranges, and the loading history varied simultaneously across the five discs.

The performance of GP was found to vary for different kernel and length scale selections and there was no uncertainty related to the original constitutive model, temperature reconstruction, geometry, or crack detection included in the nominal intervals. Therefore, coverage of four cases should not be interpreted as statistical calibration.

Comparison with Previous Studies

The present study is compared with related deformation-based and Gaussian-process fatigue study in terms of dataset, purpose, and main finding as shown in Table 6.

Table 6. Comparison with Related Fatigue-Life Studies.

Study	Dataset and purpose	Main finding
Getsov et al. [1]	Five turbine discs; deformation-based crack-initiation life prediction	Outperformed the Manson relation; present recalculation gave MAE = 8.0 and RMSE = 11.9 cycles.
Karolczuk and Słoński [13]	Multiaxial fatigue data; direct GP life prediction	Demonstrated GP applicability using critical-plane variables.
Karolczuk et al. [14]	Proportional and non-proportional loading; direct GP modeling	Showed that representative training cases strongly influence prediction accuracy.
Karolczuk et al. [15]	Multiaxial loading with static components	Used physical constraints to reduce nonphysical GP predictions.
Gao et al. [16]	328 cases from 12 metallic materials; remaining-life prediction	Applied GP to a substantially larger and more diverse dataset.
Present study	Five turbine-disc cases; residual correction	GP reduced MAE and RMSE to 4.9 and 6.9 cycles, while the linear model achieved 2.2 and 2.4 cycles.

In previous studies, Gaussian processes have been applied primarily as direct fatigue-life models with larger datasets. Here, GP regression corrects an existing deformation-based prediction and it's shown that greater model complexity does not necessarily improve performance with only five cases.

5. Conclusion

This study compared constant-bias, linear, and Gaussian-process corrections to the deformation-based crack-initiation life predictions for five gas-turbine discs. The Gaussian-process correction improved the deformation-based predictions, but did not outperform the two-input linear model when evaluated with leave-one-disc-out analysis. This suggests that for the available cases, the added complexity of the Gaussian process is not yet clearly justified. The deformation criterion yielded a mean absolute error (MAE), root mean square error (RMSE), and mean absolute percentage error (MAPE) of 8.0 cycles, 11.9 cycles, and 15.3%, respectively. These were reduced by the Gaussian-process correction to 4.9 cycles, 6.9 cycles, and 11.9%, respectively, with four cases within the nominal intervals. The linear model, however, yielded lower errors, and the sensitivity analysis yielded Gaussian-process MAEs of 2.6 to 7.4 cycles. These findings indicate that five cases are insufficient for establishing Gaussian-process superiority or general predictive validity. The damage analysis also revealed that different damage mechanisms can cause the same total damage. In some cases one sided creep accumulation dominated, in others cyclic creep played a more important part. This highlights the importance of considering individual damage components when interpreting crack-initiation behavior. In general, the study is a practical and reproducible way for the comparison of residual-correction methods without replacing the underlying deformation criterion. Further assessment will require additional independent disc cases covering a wider range of materials, geometries, temperatures, strain levels, and loading histories.

REFERENCES

[1] A. Arkhipov, Y. Ravikovich, D. Kholobtsev, and A. Shakhov, "Calculation and experimental study of low-cycle fatigue of gas turbine engines booster drum," Inventions, vol. 7, no. 3, Art. no. 49, 2022, doi: 10.3390/inventions7030049.

[2] E. J. Cross, T. J. Rogers, D. J. Pitchforth, S. J. Gibson, S. Zhang, and M. R. Jones, "A spectrum of physics-informed Gaussian processes for regression in engineering," Data-Centric Engineering, vol. 5, Art. no. e8, 2024, doi: 10.1017/dce.2024.2.

[3] J. Gao, C. Wang, Z. Xu, J. Wang, S. Yan, and Z. Wang, "Gaussian process regression based remaining fatigue life prediction for metallic materials under two-step loading," International Journal of Fatigue, vol. 158, Art. no. 106730, 2022, doi: 10.1016/j.ijfatigue.2022.106730.

[4] L. B. Getsov, A. S. Semenov, and I. A. Ignatovich, "Thermal fatigue analysis of turbine discs on the base of deformation criterion," International Journal of Fatigue, vol. 97, pp. 88–97, 2017, doi: 10.1016/j.ijfatigue.2016.12.018.

[5] S. Issler and E. Roos, "Numerical and experimental investigations into life assessment of blade-disc connections of gas turbines," Nuclear Engineering and Design, vol. 226, no. 2, pp. 155–164, 2003, doi: 10.1016/S0029-5493(03)00192-4.

[6] A. Karolczuk, Y. Liu, K. Kluger, S. Derda, D. Skibicki, and Ł. Pejkowski, "Physics-constrained Gaussian process for life prediction under in-phase multiaxial cyclic loading with superposed static components," International Journal of Fatigue, vol. 175, Art. no. 107776, 2023, doi: 10.1016/j.ijfatigue.2023.107776.

[7] A. Karolczuk, D. Skibicki, and Ł. Pejkowski, "Gaussian process for machine learning-based fatigue life prediction model under multiaxial stress-strain conditions," Materials, vol. 15, no. 21, Art. no. 7797, 2022, doi: 10.3390/ma15217797.

[8] A. Karolczuk and M. Słoński, "Application of the Gaussian process for fatigue life prediction under multiaxial loading," Mechanical Systems and Signal Processing, vol. 167, Art. no. 108599, 2022, doi: 10.1016/j.ymssp.2021.108599.

[9] M. C. Kennedy and A. O'Hagan, "Bayesian calibration of computer models," Journal of the Royal Statistical Society: Series B (Statistical Methodology), vol. 63, no. 3, pp. 425–464, 2001, doi: 10.1111/1467-9868.00294.

[10] D. Kim, D.-Y. Kim, T. Ko, and S. H. Lee, "Physics-informed Gaussian process regression model for predicting the fatigue life of welded joints," International Journal of Fatigue, vol. 190, Art. no. 108644, 2025, doi: 10.1016/j.ijfatigue.2024.108644.

[11] X.-P. Niu, R.-Z. Wang, D. Liao, S.-P. Zhu, X.-C. Zhang, and B. Keshtegar, "Probabilistic modeling of uncertainties in fatigue reliability analysis of turbine bladed disks," International Journal of Fatigue, vol. 142, Art. no. 105912, 2021, doi: 10.1016/j.ijfatigue.2020.105912.

[12] Y. Rae, A. Benaarbia, J. Hughes, and W. Sun, "Experimental characterisation and computational modelling of cyclic viscoplastic behaviour of turbine steel," International Journal of Fatigue, vol. 124, pp. 581–594, 2019, doi: 10.1016/j.ijfatigue.2019.01.022.

[13] C. E. Rasmussen and C. K. I. Williams, Gaussian Processes for Machine Learning. Cambridge, MA, USA: MIT Press, 2006.

[14] K. M. Tomevenya and S. Liu, "Probabilistic fatigue-creep life reliability assessment of aircraft turbine disk," Journal of Mechanical Science and Technology, vol. 32, no. 11, pp. 5127–5132, 2018, doi: 10.1007/s12206-018-1010-2.

[15] R.-Z. Wang, H.-H. Gu, S.-P. Zhu, K.-S. Li, J. Wang, X.-W. Wang, H. Miura, X.-C. Zhang, and S.-T. Tu, "A data-driven roadmap for creep-fatigue reliability assessment and its implementation in low-pressure turbine disk at elevated temperatures," Reliability Engineering & System Safety, vol. 225, Art. no. 108523, 2022, doi: 10.1016/j.ress.2022.108523.

[16] X. Yang, D. Barajas-Solano, G. Tartakovsky, and A. M. Tartakovsky, "Physics-informed CoKriging: A Gaussian-process-regression-based multifidelity method for data-model convergence," Journal of Computational Physics, vol. 395, pp. 410–431, 2019, doi: 10.1016/j.jcp.2019.06.041.

[17] S.-P. Zhu, Q. Liu, W. Peng, and X.-C. Zhang, "Computational-experimental approaches for fatigue reliability assessment of turbine bladed disks," International Journal of Mechanical Sciences, vols. 142–143, pp. 502–517, 2018, doi: 10.1016/j.ijmecsci.2018.04.050.